Catal Lett (2012) 142:1211–1217
DOI 10.1007/s10562-012-0894-1

# Vacancy-Driven Surface Segregation in $Ni_xMg_{1-x}O(100)$ Solid Solutions from First Principles Calculations

**Daniel Torres · Ping Liu**

Received: 17 May 2012 / Accepted: 16 August 2012 / Published online: 5 September 2012


**Abstract** Reduced $Ni_xMg_{1-x}O$ solid solutions are promising catalytic materials for the dry reforming of methane with carbon dioxide, a reaction of tremendous importance that converts two green-house gases into syngas. Conventional nickel-based catalysts have been found to encounter carbon deposition (i.e., coking), one of the major resources that cause the catalyst deactivation. Previous studies suggested that MgO-supported Ni nanoparticles produced from the reduction of $Ni_xMg_{1-x}O$ can inhibit the accumulation of carbon. The efficiency and durability of the catalyst strongly depends on the morphology. Here we employed density functional theory to investigate the structural changes of the $Ni_xMg_{1-x}O(100)$ solid solution under different conditions. Our results show that Ni ions preferentially anti-segregate to the subsurface layers of the MgO matrix during the NiO–MgO intermixing. Under reducing conditions, Ni ions facilitates the generation of oxygen vacancies, which prefer to couple together with Ni ions inside the MgO matrix to form a Ni ion–oxygen vacancy pair. In addition, the segregation of a Ni ion–oxygen vacancy pair can be controlled by changing the concentrations of Ni ions. This is driven by the strong interaction between oxygen vacancies and Ni ions. It is well known that oxygen vacancies play an important role during a catalytic reaction on an oxide, providing active sites to help the adsorption and dissociation of reaction intermediates. Our results show that in mixed oxides oxygen vacancies could also drive the segregation of the catalytically active components and provide new opportunities to tune the catalytic activity of oxides.

D. Torres · P. Liu (✉)
Center for Functional Nanomaterials, Brookhaven National Laboratory, Upton, NY 11973, USA
e-mail: pingliu3@bnl.gov

**Keywords** Mixed oxides · Segregation · NiO–MgO · Oxygen vacancy · DFT

## 1 Introduction

Mixed-metal oxides have recently re-emerged as very attractive materials in many applications such as photoelectronics, fuel cells or catalysis [1–5]. It has been found that the interaction between the oxides in the mixture may allow a fine-tuning of the properties of each other and therefore results in a superior activity over the individuals. Solid oxide solutions—solid-state mixtures of one or more oxides (solutes or dopant agents) in an oxide solvent (host matrix)—are particularly interesting. NiO–MgO solid solutions have been widely used as catalysts for methane activations, in particular, dry reforming of methane. Methane dry reforming, $CO_2 + CH_4 \rightarrow 2CO + 2H_2$, combines two of the most problematic greenhouse gases to generate syngas for the synthesis of clean liquid fuels and valuable chemicals. In industry, Ni-based catalysts have been used for methane dry reforming as they are relatively cheap and exhibit high conversion [6, 7]; yet, due to the high-temperature reaction of the reforming process, the conventional Ni catalysts deactivate quickly due to sintering of the active metal phase and carbon deposition (i.e., coking) [8, 9]. Currently, there is no commercial catalyst robust enough to sustain dry reforming reactions on an industrial scale. The catalysts based on noble metals have been reported to be less sensitive to coking than the nickel-based catalysts. However, considering the high cost and limited availability of noble metals [10], it is more profitable to develop a Ni-based catalyst, which is resistant to carbon accumulation and exhibits long-term stability. It has been shown that the interaction between Ni and an oxide or

a mixed oxide support exerts a great effect on its catalytic properties as well as inhibiting carbon deposition [11–14]. As an example of this, previous studies demonstrated that an oxide support affects the nucleation mechanism and even the magnetic state of small Ni clusters [15–17]. In particular, reduced NiO–MgO solid solutions have been reported to exhibit a high stability against metal sintering and a strong coking resistance [18–22]. Unfortunately, there is no clear explanation behind the unusual behavior of the reduced $Ni_xMg_{1-x}O$ catalyst.

One of the keys to control the performance of the catalyst is the preparation procedure. Factors such as the solute composition or the reduction conditions sensitively affect the activity and stability of the catalyst. Reducing $Ni_xMg_{1-x}O$ catalysts in a hydrogen atmosphere at high temperature has been found to result in well-dispersed Ni particles inside the MgO matrix [23]. Effects of precursor concentration are also important, and relatively low NiO contents, in the range 9.2–28.6 wt%, have been found to be effective to achieve a highly active catalyst [24]. Another key factor is associated with the oxygen vacancies produced during the reduction [25]. Oxygen vacancies are known to affect the catalytic properties of oxides by directly participating in the reaction and helping to adsorb and dissociate reaction intermediates [26]. For the reduced $Ni_xMg_{1-x}O$, oxygen vacancies have been proposed to drive the segregation of small amounts of Ni from the matrix to the solid–gas interface, which could be responsible for the high activity and stability of the catalyst during methane dry reforming [6]. Significant research efforts have been made addressing the thermodynamics of segregation on ideal metal alloy surfaces [27]. However, little is known about the strength of surface segregation in mixed oxides, which is important for catalytic applications. The fundamental understanding of $Ni_xMg_{1-x}O$ has so far been limited to the adsorption of a Ni atom on or in the surface layer of MgO(100) [28–30]. A deeper understanding of the atomic arrangement of the Ni ions in the MgO matrix during the intermixing and reduction remains elusive, which will help unravel the principles that underlie the catalytic performance of the oxide.

Here we employ Density Functional Theory (DFT) to investigate the structural changes of $Ni_xMg_{1-x}O$ solid solutions under different conditions. Our calculations reveal that during the intermixing, Ni ions preferentially anti-segregate to the subsurface of $Ni_xMg_{1-x}O$ and hence the surface is terminated by MgO. Oxygen vacancies, created during the early stages of the oxide reduction, trigger the segregation of the active components. According to our calculations, an active Ni ion and an oxygen vacancy are coupled together and form a pair. The pair prefers to stay on the surface of the oxide matrix at relatively low Ni concentration and in the subsurface at relatively high Ni concentration. The vacancy-driven segregation is attributed to the strong association of oxygen vacancies and Ni ions, and can have a significant effect on the performance of the reduced $Ni_xMg_{1-x}O$ catalysts for methane dry reforming.

## 2 Methodology

The intermixing of NiO with a rock-salt-based MgO matrix was studied using DFT, which was implemented with the Vienna Ab Initio Simulation Package [31–34]. The spin-polarized generalized gradient approximation with the PW91 functional and pseudopotentials generated in the projector-augmented wave method were employed. An energy cutoff of 400 eV ensured planewave convergence, and the Brillouin zone integration was performed on a $7 \times 7 \times 1$ Monkhorst–Pack grid for all Ni–Mg–O compounds or a $12 \times 12 \times 12$ grid for bulk materials [35]. The convergence criterion was an atomic force of 10 meV/Å. We focus on the $Ni_xMg_{1-x}O$ mixtures, where "$x$" is the concentration of Ni with $x = 0.04$, 0.08, 0.12 and 0.16 (or 7.4, 14.4, 20.9 and 27.0 wt%). In this concentration range, $Ni_xMg_{1-x}O$ mixtures have been reported to be paramagnetic [36]. Hence, our computational approach is enough to adequately describe the magnetic and electronic structure of the mixtures. A six-layer slab with a $(2 \times 2)$ unit cell, as shown in Fig. 1, was used to model the MgO(100) matrix, being part of the Mg ions were replaced by Ni ions. The total energy of the mixtures was minimized with the full relaxation of the atomic positions of the three topmost oxide layers, whereas the three bottom layers were fixed to their bulk PW91-optimal positions ($a_{MgO} = 4.237$ Å). Our results indicated that Ni ions retain the magnetization, being the average magnetic moment of two BM.

We used two relevant thermodynamic potentials in order to study the surface segregation and reduction of the $Ni_xMg_{1-x}O$ solid solution. We computed the surface segregation energy, $E_{segr}$, defined per supercell as follows in Eq 1.

$$E_{segr} = E[Ni_xMg_{1-x}O(100)] - E\left[Ni_xMg_{1-x}O(100)_{surf}\right] \quad (1a)$$

for fully oxidized $Ni_xMg_{1-x}O$. Or.

$$E_{segr} = E[Ni_xMg_{1-x}O_{0.96}(100)] - E\left[Ni_xMg_{1-x}O_y(100)_{surf}\right] \quad (1b)$$

for $Ni_xMg_{1-x}O_{0.96}$ with one oxygen vacancy per supercell. E is the total energy per supercell of the corresponding slabs ($Ni_xMg_{1-x}O(100)$: Ni ions at different layers; $Ni_xMg_{1-x}O(100)_{surf}$: Ni ions only on the surface layer; $Ni_xMg_{1-x}O_y(100)$: both Ni ions and the oxygen vacancy on its most stable position; $Ni_xMg_{1-x}O_y(100)_{surf}$: both Ni ions

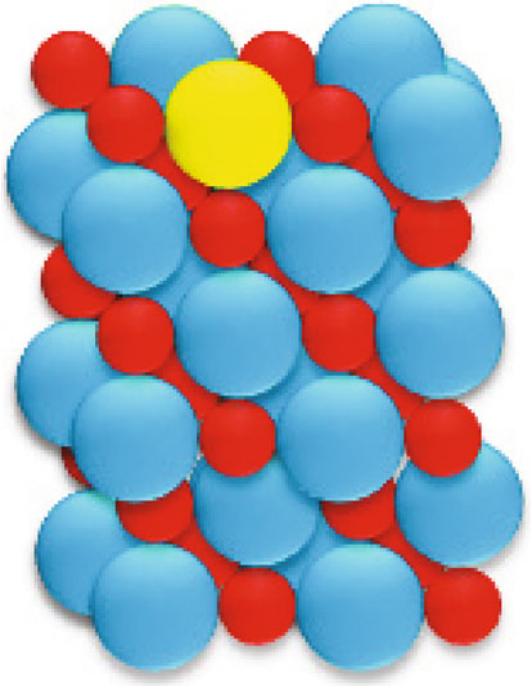

**Fig. 1** Schematic representation of a supercell of $Ni_xMg_{1-x}O(100)$ model ($x = 0.04$). The *red* spheres represent oxygen atoms whereas the *blue* and *yellow* spheres represent the Mg and Ni cations, respectively

and the oxygen vacancy on the surface layer). $E_{segr}$ is a reasonable estimate of the tendency of segregation of Ni ions to the surface. We also computed reduction Gibbs free energies associated to the following defect-mediated process.

$$O^{2-} + Ni^{2+} + H_{2(g)} \rightarrow V^{\delta-} + Ni^{\delta+} + H_2O_{(g)} \quad (2)$$

where the superscript represents the charge of an ion and V stands for an oxygen vacancy. The value of $\delta$ is between zero and two. Reduction Gibbs free energies, $\Delta G^{\circ}_{Red}$, were calculated at 700 K and computed at standard pressure conditions according to Eq. 3.

$$\begin{aligned}\Delta G^{\circ}_{Red} &= G^{\circ}_{Products} - G^{\circ}_{Reactants} = \Delta H^{\circ}_{Red} - T\Delta S^{\circ} \\ &\approx E(Ni_xMg_{1-x}O_{0.96}) - E(Ni_xMg_{1-x}O) \\ &\quad - T(S^{\circ}_{H_2O} - S^{\circ}_{H_2})\end{aligned} \quad (3)$$

where T and $k_B$ are respectively the temperature and Boltzmann constant. The standard enthalpy change, $\Delta H^{\circ}_{Red}$, can be approximated with the total energy change per supercell neglecting the PV term, and the standard entropy change, $\Delta S^{\circ}$, is dominated by the change in entropy contribution of the gas phase $H_2O$ ($S^{\circ}_{H_2O}$) and $H_2$ ($S^{\circ}_{H_2}$), being much higher than that of condensed phases or configurational entropy of the solid solution ($\sim$0.64 meV/K vs. $\sim$–0.02 meV/K per oxide unit formula). The entropy contribution was calculated on the basis of atomistic thermodynamics [37]. Reduction free energies were translated to reduction temperatures for $p_{H_2O}/p_{H_2} = 10^{-5}$ and for equilibrium conditions ($\Delta G^{\circ}_{Red} = 0$).

## 3 Results

We first address the structure for $Ni_xMg_{1-x}O$ oxide solutions and analyse the thermodynamics of oxide-mixing. A key quantity of interest is $E_{segr}$, which determines the tendency of segregation of Ni ions to the surface. $E_{segr}$ depends on the solute (Ni ion) concentration and distribution in the matrix. For each solute concentration, we consider a set of different solute positions leading to different layer population. For sufficiently negative segregation energies, the surface layer will contain the Ni ion, whereas if the energy of segregation is positive, the surface layer is mostly MgO-terminated.

Figure 2 displays the $E_{segr}$ as expressed in Eq. 1 for different solute configurations. The set of configurations displayed along the X axis represents the anti-segregation of solute from the topmost surface layer to the second and the third layer in the subsurface at different concentrations of solute. Our results indicate that the distribution of solute inside the MgO matrix is not uniform. As shown in Fig. 2, at all four concentrations, Ni ions prefer the near-surface region of the matrix (the second layer) instead of the top surface layer or the bulk-like third layer. This anti-segregation can be rationalized by means of surface energy. The surface energy of MgO is lower compared to that of NiO ($\gamma_{MgO} = 2.38$ J/m$^2$ and $\gamma_{NiO} = 5.34$ J/m$^2$ [38]). Anti-segregation of NiO to the second layer of the matrix is able to reduce the surface energy of the mixture. In contrast, the further migration of Ni ions to the third layer is less favourable. According to the previous studies [39, 40], the low-coordinated oxygen ion on MgO is more active than the high-coordinated. In the case of $Ni_xMg_{1-x}O(100)$, the Ni ions in the third layer only interact with the bulk oxygen ions with coordination of six; in contrast, the Ni ions in the second layer is able to interact with a low-coordinated oxygen ion in the surface (coordination number, five), which provides a stronger binding than those in the bulk. In this way, a NiO-free surface is likely to form on a fully oxidized $Ni_xMg_{1-x}O(100)$ mixture.

The next question is what the effects of reduction on the $Ni_xMg_{1-x}O$ structure are and whether the presence of a single oxygen vacancy generated during the reduction will affect the structure of the mixed oxide. $Ni_xMg_{1-x}O$ is reduced through the creation of oxygen vacancies (see Eq 2). The electronic structure of an oxygen vacancy associated to a Ni cation on a NiO matrix has been previously investigated theoretically, showing that the association lead to effective reduction of the Ni cation [41]. In

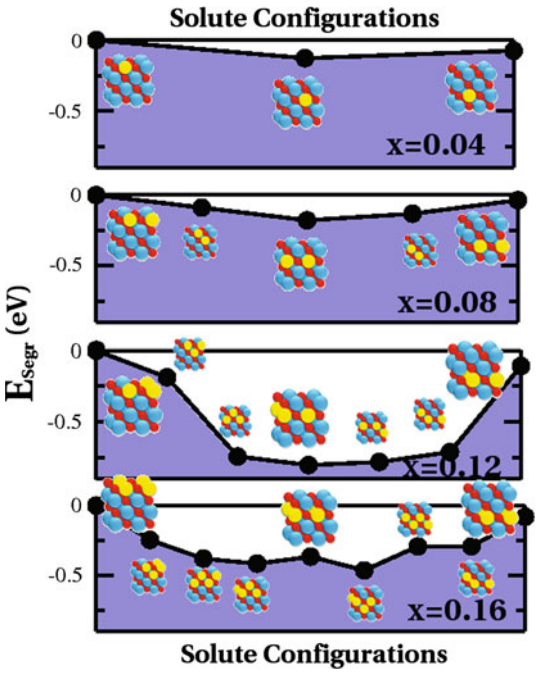


**Fig. 2** $E_{segr}$ per supercell for various solute configurations, representing the segregation of solute (Ni ion) from the topmost surface layer to the second and the third layer in the subsurface of fully oxidised $Ni_xMg_{1-x}O(100)$ mixtures with $x$ ranging from 0.04 to 0.16. We include in the inset atomistic representations of the slab models, showing only the four topmost layers of a six-layer slab. *Blue* Mg; *yellow* Ni; *red* O

the case of $Ni_xMg_{1-x}O$, the two electrons generated on creating an oxygen vacancy are delocalized between the oxygen-vacancy site and the Ni cations. In this way, Ni cations are partially reduced, which is shown in Fig. 3 for the projected density of states for a Ni cation before and after reduction. One can see that the new density of states right below the Fermi level emerges for the Ni cation after the generation of an oxygen vacancy. Therefore, as we can see in the following, the segregation behavior of those species is anticipated to be different than fully reduced Ni cation. In the present study, we only consider the creation of a single oxygen vacancy in the supercell following Eq 2. The corresponding energy is expressed in the form of reduction Gibbs free energies $\Delta G^{\circ}_{Red}$ per supercell and is displayed in Fig. 4 for different solute concentrations. For each solute concentration, $\Delta G^{\circ}_{Red}$ is calculated based on the configuration with the most stable position for the solute, which is shown in Fig. 5 together with other less stable structures and energetics. We understand the vacancy concentration should be larger under reducing environments. What we are focusing now is on the initial reduction process. We use $\Delta G^{\circ}_{Red}$ to scale the redox properties of the oxide and the reduction is thermodynamically more favourable with the lower Gibbs energy [42]. The calculated $\Delta G^{\circ}_{Red}$ value for MgO(100) is $\sim$3.4 eV, which corresponds to a reduction temperature of T $\sim$ 2300 K. This is in qualitative agreement with the experimental evidence, finding a reduction temperature of $\sim$2500 K [43]. Our results probe that the addition of NiO facilitates the reduction of MgO. For a $Ni_xMg_{1-x}O(100)$ solid solution with $x = 0.04$, a reduction temperature of 1900 K is estimated, which corresponds to a $\Delta G^{\circ}_{Red}$ value of $\sim$2.7 eV. This effect is associated with the binding strength of oxygen anions in the oxide matrix. It has been reported that the energy required to create an oxygen vacancy on NiO(100) is considerably smaller by 2 eV than that on MgO(100) [15, 44]. The presence of NiO in the MgO matrix helps decreasing the vacancy formation energy by more than 1 eV. Our calculations also indicate that the oxygen ions directly bound to Ni are easier to remove than those bound to Mg, hence suggesting that oxygen vacancies and Ni ions tend to be located close to each other and form a pair. A similar effect has recently been found for the mixtures of reducible oxides, e.g., ceria and titania [45]. Figure 4 also shows that the dependence of $\Delta G^{\circ}_{Red}$ on the solute concentration, which is in agreement with experimental studies [46]. The reduction energy decreases as the amount of Ni ions increases and consequently reduction temperature is lowered. With the increasing of Ni concentration from x = 0.04 to x = 0.16, $\Delta G^{\circ}_{Red}$ for $Ni_xMg_{1-x}O$ mixed oxide is reduced by more than 2 eV (Fig. 4) and the reduction temperature is decreased by $\sim$1600 K down to $\sim$300 K.

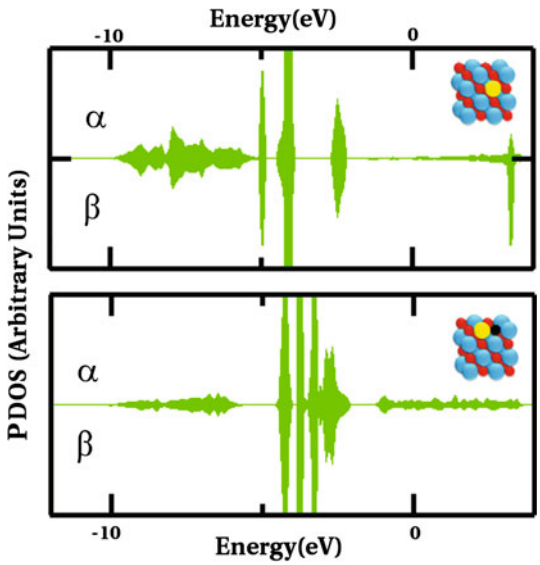


**Fig. 3** Projected density of states (LDOS) to a Ni cation in the fully oxidised (Top Panel) and the reduced $Ni_xMg_{1-x}O(100)$ mixture with a single oxygen vacancy (Bottom Panel), where $x$ = 0.04 and 3d, 4s and 4p orbitals are also included. The zero corresponds to the vacuum level. *Insets* are the corresponding configurations. *Blue* Mg; *yellow* Ni; *red* O; *black* $O_{vac}$

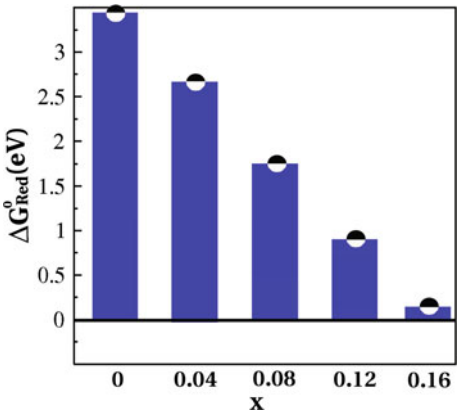


**Fig. 4** Variation in the reduction Gibbs free energies ($\Delta G^{\circ}_{Red}$) of creating a single oxygen vacancy with in $Ni_xMg_{1-x}O(100)$ unit cell with the increasing of x from 0 to 0.16. For each solute concentration, the $\Delta G^{\circ}_{Red}$ is calculated based on the configuration with the most stable position for the solute, which is shown in Fig. 4 together with other less stable structures and energetics. The lower $\Delta G^{\circ}_{Red}$ the more favoured the reduction of the mixed oxide will be

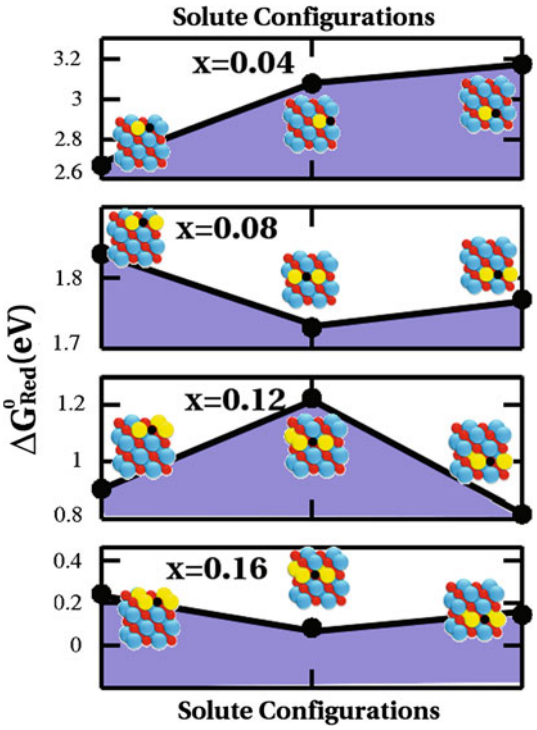


**Fig. 5** Variation in the reduction Gibbs free energies ($\Delta G^{\circ}_{Red}$) of creating a single oxygen vacancy with in $Ni_xMg_{1-x}O(100)$ supercell with the increasing of x from 0 to 0.16. For each Ni concentration, the oxygen vacancy goes from the surface layer to the second and the third layer in the subsurface along the horizontal axis. $\Delta G^{\circ}_{Reds}$ for those with the most stable arrangement of Ni corresponding to a certain position of an oxygen vacancy is shown together with the corresponding configuration. *Blue*: Mg; *yellow*: Ni; *red*: O; *black*: $O_{vac}$

Our results further suggest that a single oxygen vacancy produced during reduction can cause the segregation or anti-segregation of solute Ni ions. Figure 5 further illustrates the effect of an oxygen vacancy on $\Delta G^{\circ}_{Red}$ and the segregation of $Ni_xMg_{1-x}O(100)$. For each Ni concentration, the oxygen vacancy goes from the surface layer to the second and the third layer in the subsurface along the X-axis. $\Delta G^{\circ}_{Reds}$ for those with the most stable Ni corresponding to a certain position of the oxygen vacancy are shown together with the corresponding configuration. For a $Ni_xMg_{1-x}O$ mixture with $x = 0.04$, the Ni ion-oxygen vacancy pair prefers to be in the surface layer of the matrix, and hence the Ni ions segregate to the surface. This is in contrast to fully oxidized $Ni_xMg_{1-x}O$ mixtures, where the Ni ion preferentially incorporates in the subsurface of the matrix. The segregation effect depends on the solute concentration. With $x$ increasing to 0.08 and higher, the Ni ion–oxygen vacancy pair remains buried below the surface (Fig. 5). In order to quantify the above effect, we display in Fig. 6 $E_{segr}$ for the most stable configuration at each Ni concentration. Again, the negative energies represent for the surface containing the Ni ion–oxygen vacancy pair, and the positive energies correspond to a MgO-terminated surface. One can see that for the fully oxidized $Ni_xMg_{1-x}O$ in the whole range of solute concentrations we studied, $E_{segr}$ is positive. Differently, for the case of $Ni_xMg_{1-x}O$ in the presence of an oxygen vacancy, $E_{segr}$ varies in sign from negative to positive when going from low to high Ni concentrations.

Segregation is a common phenomenon observed in metal alloys that modifies the surface composition and therefore results in a unique catalytic activity different from that of each individual [47, 48]. The present study shows that similar effects happen for mixed oxides, though the situation is more complicated. For fully oxidized $Ni_xMg_{1-x}O(100)$, the Ni ions at different concentrations preferentially anti-segregate to the subsurface layers of the MgO matrix, rather than staying in the surface layer. Therefore, a MgO-terminated $Ni_xMg_{1-x}O(100)$ surface is likely to form; yet the presence of Ni ions in the MgO

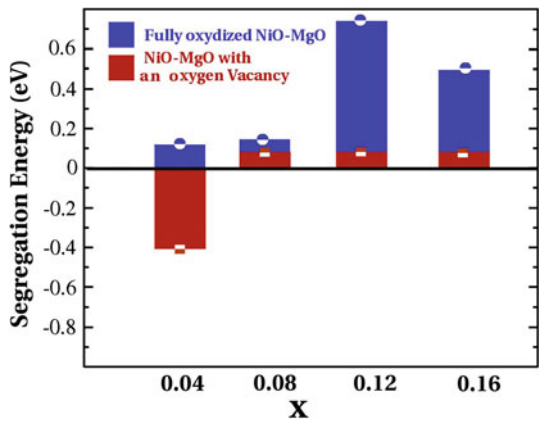


**Fig. 6** Segregation energies per supercell, $E_{segr}$ at different solute (Ni ion) concentrations for fully oxidised (*blue* bars) and reduced (*red* bars) $Ni_xMg_{1-x}O(100)$ with the increasing of $x$ from 0.04 to 0.16

matrix does facilitate the reduction process. Different from the metal alloys, under reducing conditions, the segregation in the mixed oxide varies due to the generation of oxygen vacancies. For the reduced $Ni_xMg_{1-x}O(100)$, the Ni ion–oxygen vacancy pair can stay on the surface at relatively low Ni concentrations and in the subsurface at relatively high Ni concentrations. That is, by tuning the concentrations, Ni ions and oxygen vacancies in the reduced $Ni_xMg_{1-x}O(100)$ can either be driven to the surface to participate in the reaction directly, or stay in the subsurface and play the secondary role. Accordingly, the fully oxidized $Ni_xMg_{1-x}O$ may not be catalytically active towards methane dry reforming due to the presence of non-reducible or relatively inert MgO on the surface; in contrast, the reduced $Ni_xMg_{1-x}O$ favours the partially reduced Ni ions and oxygen vacancies on the surface at low Ni concentration, which are much more active than MgO and therefore higher activity is likely to be achieved. We believe that this effect is driven by the nature of the vacancy-cation association. As shown in Fig. 3, the removal of an oxygen anion leaves two electrons which are delocalized between the Ni ion and the vacancy, leading to a strong vacancy-cation interaction [36]. On bare MgO, this effect does not happen and the two electrons are localized at the vacancy site. Such insights are of great importance to the development of better catalysts. A strong defect-cation interaction has been found responsible for the high ionic conductivity of other oxides such as doped ceria [49], while our present study points out the possible roles that it could play in catalysis.

## 4 Conclusions

In the present work, we investigated the surface composition of $Ni_xMg_{1-x}O$ solid solutions by means of DFT calculations. Our results revealed that, during the intermixing, Ni ions preferentially segregate to the subsurface and hence a MgO-terminated $Ni_xMg_{1-x}O(100)$ surface is likely to form. Under reducing conditions, the presence of Ni ions facilitate the generation of oxygen vacancies in the MgO matrix, where the partially reduced Ni ion and an oxygen vacancy prefer to couple together and form a pair. In addition, oxygen vacancies are able to trigger the segregation or anti-segregation of partially reduced Ni ions. Depending on the concentration of solute Ni ions, the Ni ion–oxygen vacancy pair can stay either on the surface or in the subsurface. Therefore, the $Ni_xMg_{1-x}O(100)$ surface terminated either by the relatively active oxygen vacancies and Ni ions or by the relatively inert MgO can be achieved. Accordingly, the fully oxidized $Ni_xMg_{1-x}O$ may not be catalytically active towards methane dry reforming due to the presence of relatively inert MgO on the surface; in contrast, the reduced $Ni_xMg_{1-x}O$ can display higher activity, being able to hold the active Ni ions and oxygen vacancies on the surface.This segregation is rationalized in terms of a radically strong interaction between oxygen vacancies and Ni ions.

It is well known that the catalytic activity of an oxide strongly depends on the metal ions, oxygen ions and oxygen vacancies exposed on the surface, which may participate directly in the adsorption and dissociation of the reaction intermediates. Our results suggest that for mixed oxides, the situation can be more complicated. Segregations have to be considered, which leads to the presence of different metal ion species on the surface. In addition, oxygen vacancies may not only act as active sites. The segregation of catalytically active components can also be driven by oxygen vacancies. A careful control of the conditions during the reduction of mixed oxides can potentially provide the opportunity to control the distributions of active metal ion–oxygen vacancy pairs and therefore the catalytic activity of the mixture.

**Acknowledgments** The authors are indebted to Dr. M. S. Hybertsen for stimulating discussions and for carefully reading the manuscript. This work was carried out at Brookhaven National Laboratory (BNL) under Contract No. DE-AC02-98CH10886 with the US Department of Energy, Office of Science. The calculations utilized resources at the BNL Center for Functional Nanomaterials (CFN).

## References

1. Yang L, Wang SZ, Blinn K, Liu MF, Liu Z, Cheng Z, Liu ML (2009) Science 326:126
2. Yang F, Kundu S, Vidal AB, Ramírez PJ, Senanayake SD, Stacchiola D, Evans J, Liu P, Rodriguez JA (2011) Angew Chem Int Ed 50:10198
3. Park B, Graciani J, Evans J, Stacchiola D, Ma S, Liu P, Nambu A, Fdez SJ, Hrbek J, Rodriguez JA (2009) Proc Natl Acad Sci USA 106:4975
4. Yang F, Choi Y, Agnoli S, Liu P, Stacchiola D, Hrbek J, Rodriguez JA (2011) J Phys Chem C 115:23062
5. Campbell CT, Peden CHF (2005) Science 309:713
6. Navarro RM, Pena MA, Fierro JLG (2007) Chem Rev 107:3952
7. Kroll VCH, Swaan HM, Mirodatos C (1996) J Catal 161:409
8. Rostrupnielsen JR, Hansen JHB (1993) J Catal 144:38
9. Kroll VCH, Swaan HM, Lacombe S, Mirodatos C (1996) J Catal 164:387
10. Sarusi I, Fodor K, Baán K, Oszkó A, Pótári G, Erdohelyi A (2011) Catal Today 171:132
11. Ruckenstein E, Hu YH (1995) Appl Catal A Gen 133:149
12. Kumar P, Sun Y, Idem RO (2007) Energy Fuels 21:3113
13. Cui Y, Zhang H, Xu H, Li W (2007) Appl Catal A Gen 331:60
14. Bellido JDA, De Souza JE, M'Peko J-C, Assaf EM (2009) Appl Catal A Gen 358:215
15. Di Valentin C, Giordano L, Pacchioni G, Rösch N (2003) Surf Sci 522:175
16. Giordano L, Pacchioni G, Illas G, Rösch N (2002) Surf Sci 499:73
17. Del Vitto A, Giordano L, Pacchioni G, Rösch N (2005) Surf Sci 575:103

18. Ruckenstein E, Hu YH (1995) Appl Catal A Gen 133:149
19. Ruckenstein E, Hu YH (1998) Catal Lett 51:183
20. Ruckenstein E, Hu YH (1997) Appl Catal A Gen 154:185
21. Ruckenstein E, Hu YH (1998) Catal Lett 51:183
22. Hu YH, Ruckenstein E (1997) Catal Lett 43:71
23. Martra G, Marchese L, Arena F, Parmaliana A, Coluccia S (1994) Topics Catal 1:63
24. Hu YH, Ruckenstein E (1996) Catal Lett 36:145
25. Pacchioni G (2003) Chem Phys Chem 4:1041
26. Rodriguez JA, Hanson JC, Frenkel AI, Kim JY, Perez M (2002) J Am Chem Soc 124:346
27. Ruban AV, Skriver HL, Nørskov JK (1999) Phys Rev B 59:15990
28. Yudanov I, Pacchioni G, Neyman K, Rösch N (1997) J Phys Chem B 101:2786
29. López N, Illas F (1998) J Phys Chem B 102:1430
30. Valero R, Gomes JRB, Truhlar DG, Illas F (2010) J Chem Phys 132:104701
31. Kresse G, Hafner JJ (1993) Phys Rev B 47:558
32. Kresse G, Furthmuller JJ (1996) Phys Rev B 54:11169
33. Perdew JP, Chevary JA, Vosko SH, Jackson KA, Pederson MR, Singh D, Fiolhais C (1992) Phys Rev B 46:6671
34. Blöchl P (1994) Phys Rev B 50:17953
35. Monkhost H, Pack J (1993) Phys Rev B 47:558
36. Cimino A, LoJacono M, Porta P, Valigi M (1967) Z Phys Chem 55:14
37. Llofreda D (2003) Surf Sci 600:2103
38. Wander A, Bush IJ, Harrison NM (2003) Phys Rev B 68:233405
39. Di Valentin C, Finazzi E, Pacchioni G (2005) Surf Sci 591:70
40. Giordano L, Di Valentin C, Pacchioni G, Goniakowski J (2005) Chem Phys 309:41
41. Ferrari AM, Pisani C, Cinquini F, Giordano L, Pacchioni G (2007) J Chem Phys 127:174711
42. Zhenpeng H, Horia M (2011) J Phys Chem C 115:17898
43. Schwartz M, Gershaw R, Dwight K, Wold A (1987) Mat Res Bull 22:609
44. Carrasco J, Lopez N, Illas F, Freund HJ (2006) J Chem Phys 125:074711
45. Graciani J, Plata JJ, Sanz JF, Liu P, Rodriguez JA (2010) J Chem Phys 132:104703
46. Parmaliana A, Arena F, Frusteri F, Giordano N (1990) J Chem Soc, Faraday Trans 86:2663
47. Liu P, Logadóttir Á, Nørskov JK (2003) Electrochimina Acta 48:3731
48. Shao M, Liu P, Adzic RR (2007) J Phys Chem B 111:6772
49. Wei X, Pan W, Cheng L, Li B (2009) Solid State Ionics 180:13